南京航空航天大学

Nanjing University of Aeronautics and Astronautics

Nonperturbative QCD inside the photon

史潮

(cshi@nuaa.edu.cn)

2024.07.03@中国科学技术大学《第二届强子物理新发展研讨会》

Background

- Photon is an elementary particle.
- Yet by quantum mechanics, it can be a supperposition of states with virtual particles.

$$|\gamma^*_{\rm phys}\rangle = |\gamma^*_{\rm bare}\rangle + |e^+e^-\rangle_{\gamma^*} + \sum_{f=u,d,s\ldots} |q_f\bar{q}_f\rangle_{\gamma^*} + \ldots$$

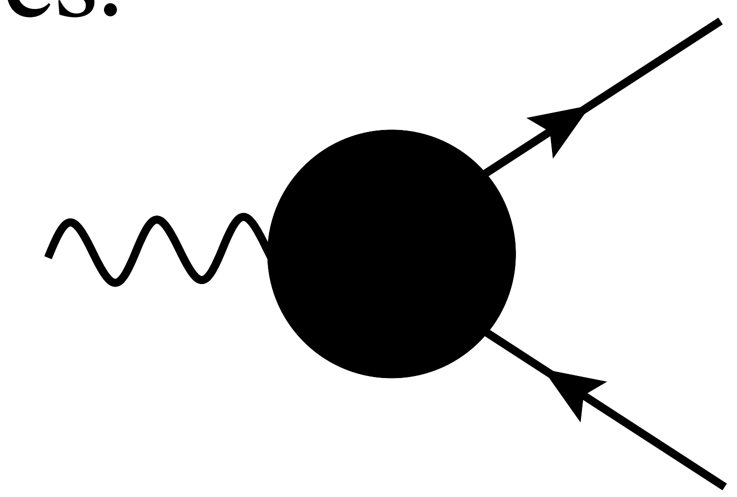

- Where there are colored objects, there is QCD effect.
- Historically, the QCD content of photon provides an early evidence of QCD.

$$R = \frac{\sigma(e^- + e^+ \rightarrow \text{hadrons})}{\sigma(e^- + e^+ \rightarrow \mu^- + \mu^+)}.$$

- The quark parton distribution in photon has been studied from various aspects, including its extraction from $e^+e^- \rightarrow e^+e^- +$ hadrons (OPAL_EPJC2000) and its impact on proton parton structure.(CTEQ-TEA_PRD2022)
- Photon LFWFs are important elements in the search of gluon saturation within color dipole approach.

Deep Inelastic Scattering

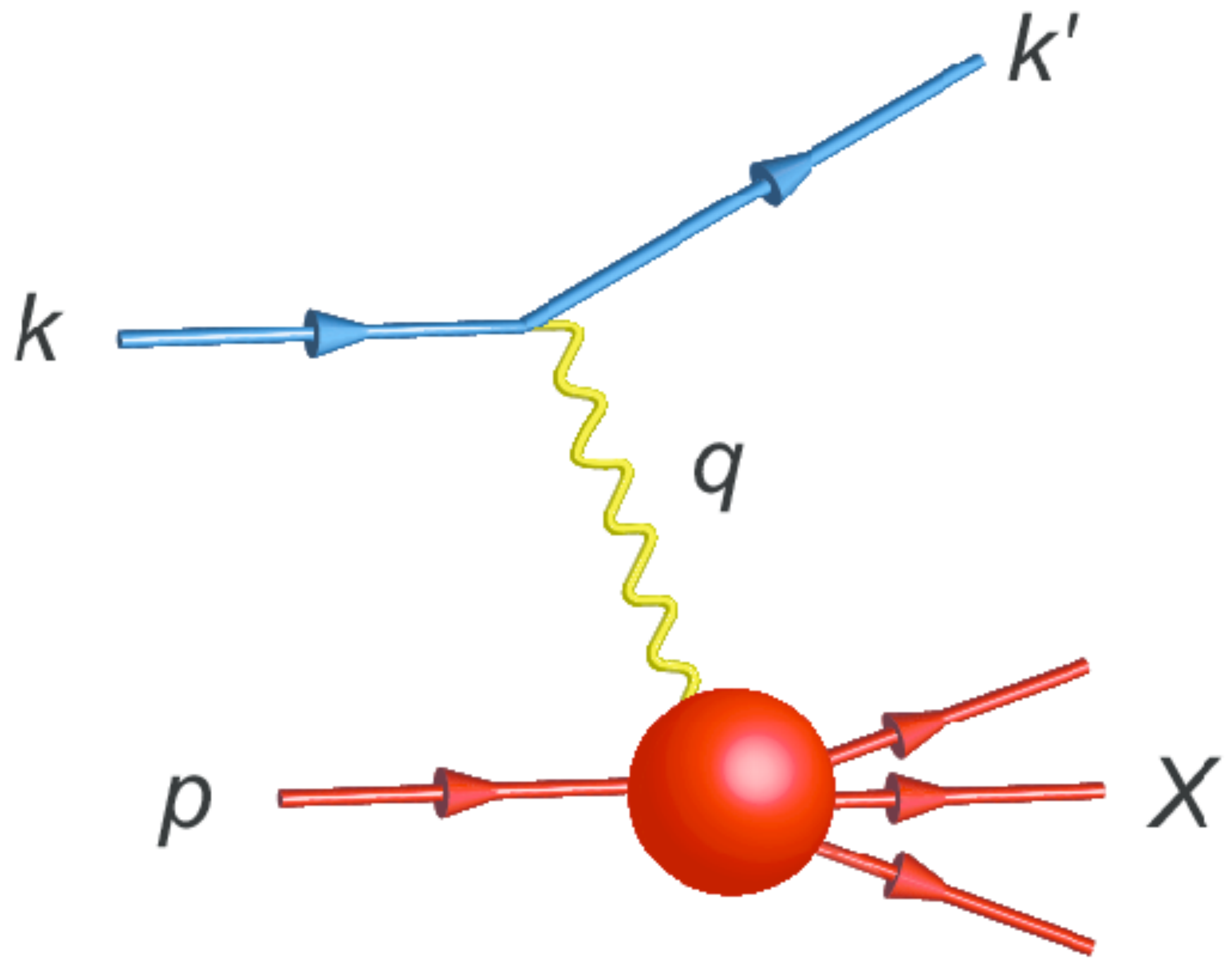

Color Dipole Model

Im {

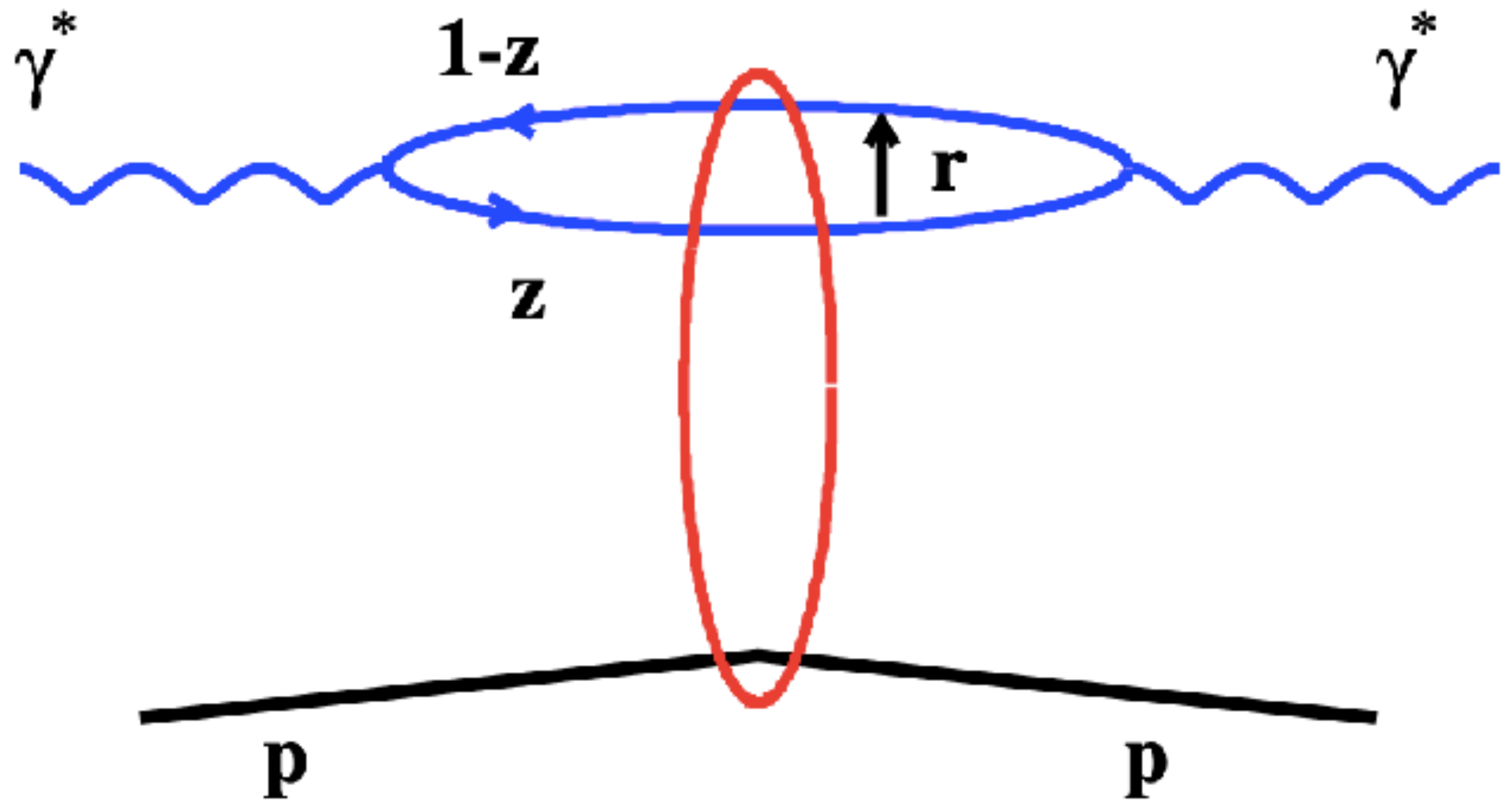

}

Kowalski_PRD2006

- Color Dipole Picture of DIS

$$\sigma \sim \left|\phi_{\gamma^*}^{q\bar{q}}\right|^2 \otimes \sigma_{q\bar{q},N}$$

$\phi_{\gamma*}^{q\bar{q}}$ photon's LFWF

$\sigma_{q\bar{q},N}$ color-dipole-nucleon scattering amplitude

Diffractive Vector Meson Production

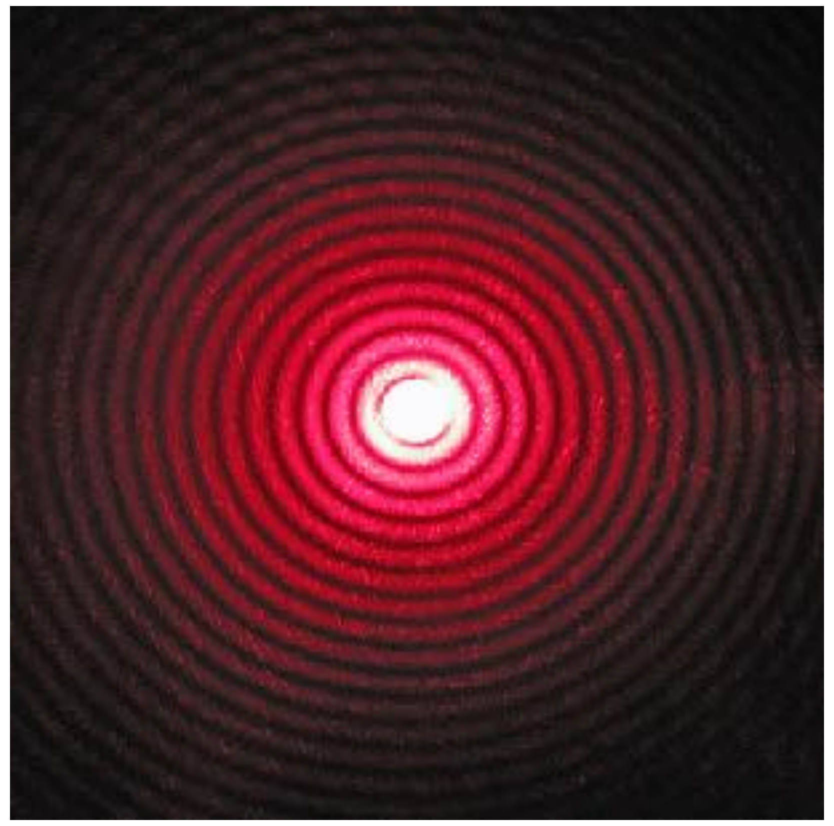

Optical Diffraction

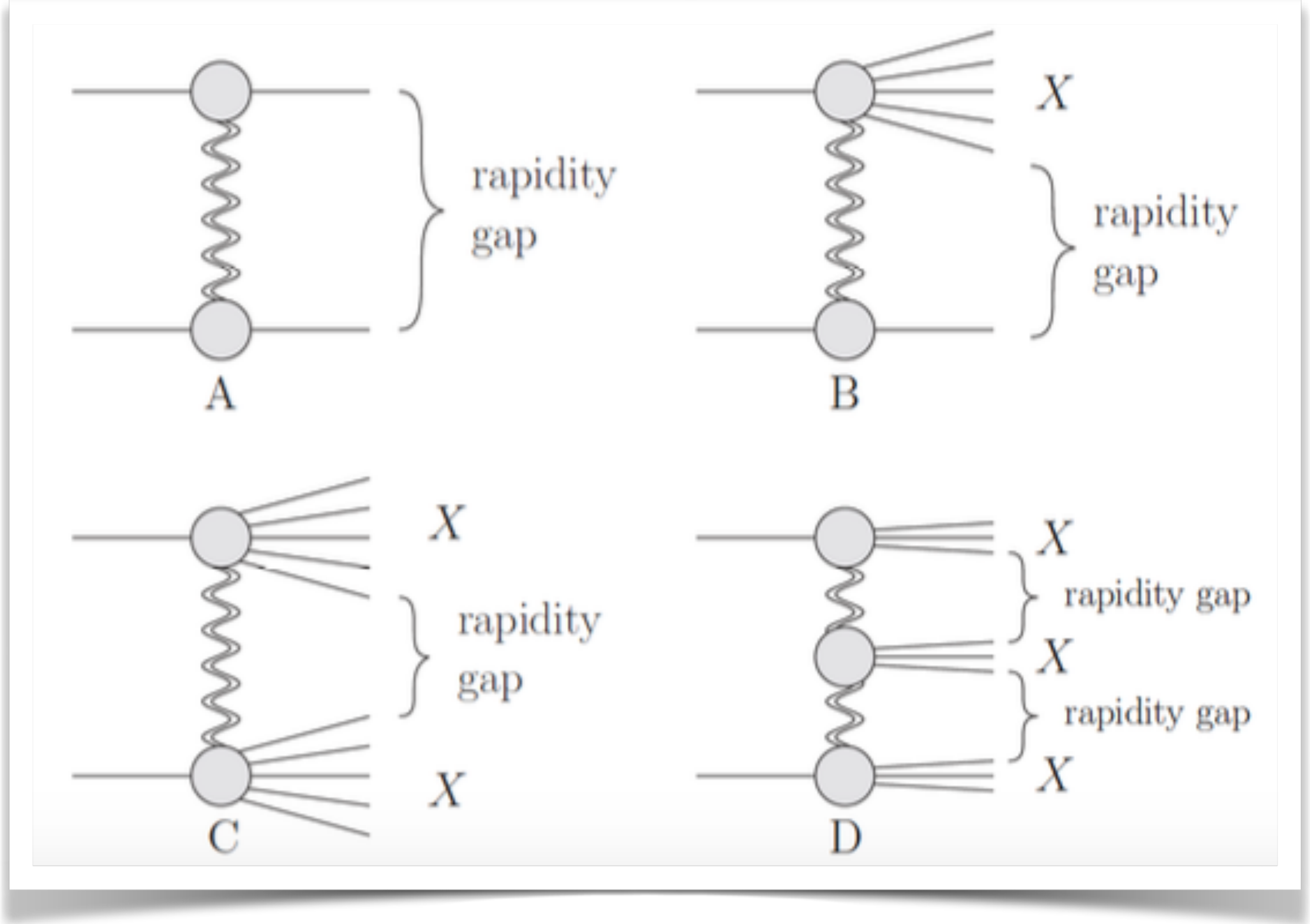

QCD diffraction. Colorless exchange

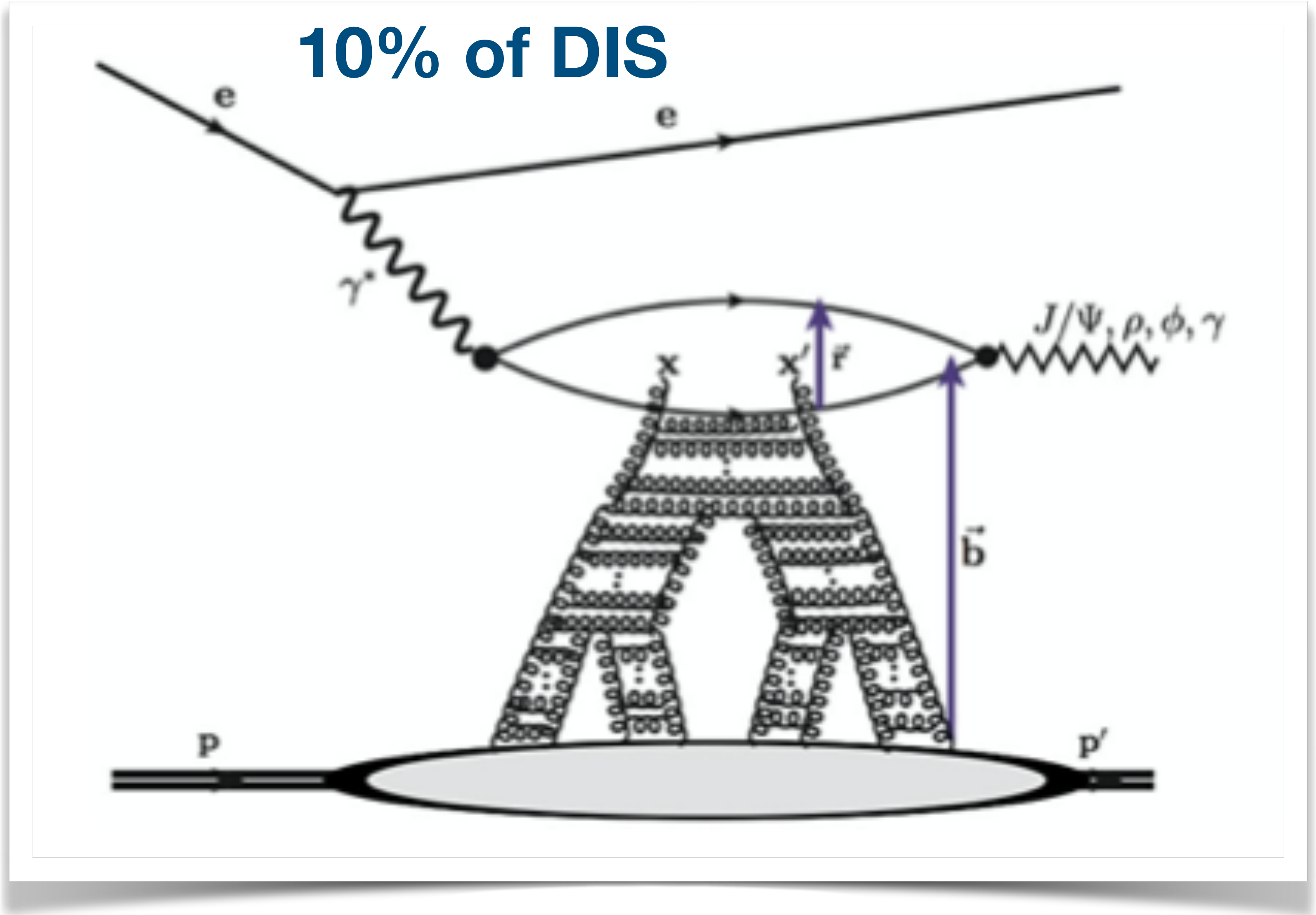

Diffractive VMP

Kowalski_PRD2006

- Color Dipole Picture of diffractive VM production

$$\sigma \sim \phi^{q\bar{q}}_{\gamma^*} \otimes \sigma_{q\bar{q},N} \otimes \phi^{q\bar{q}}_{V}$$

$\phi^{q\bar{q}}_{\gamma*}$ photon's LFWF

$\sigma_{q\bar{q},N}$ color-dipole-nucleon scattering amplitude

$\phi^{q\bar{q}}_{V}$ vector meson LFWF

Small x and gluon saturation

$$\sigma \sim |\phi_{\gamma^*}^{q\bar{q}}|^2 \otimes \sigma_{q\bar{q},N}$$

$$\sigma \sim \phi_{\gamma^*}^{q\bar{q}} \otimes \sigma_{q\bar{q},N} \otimes \phi_V^{q\bar{q}}$$

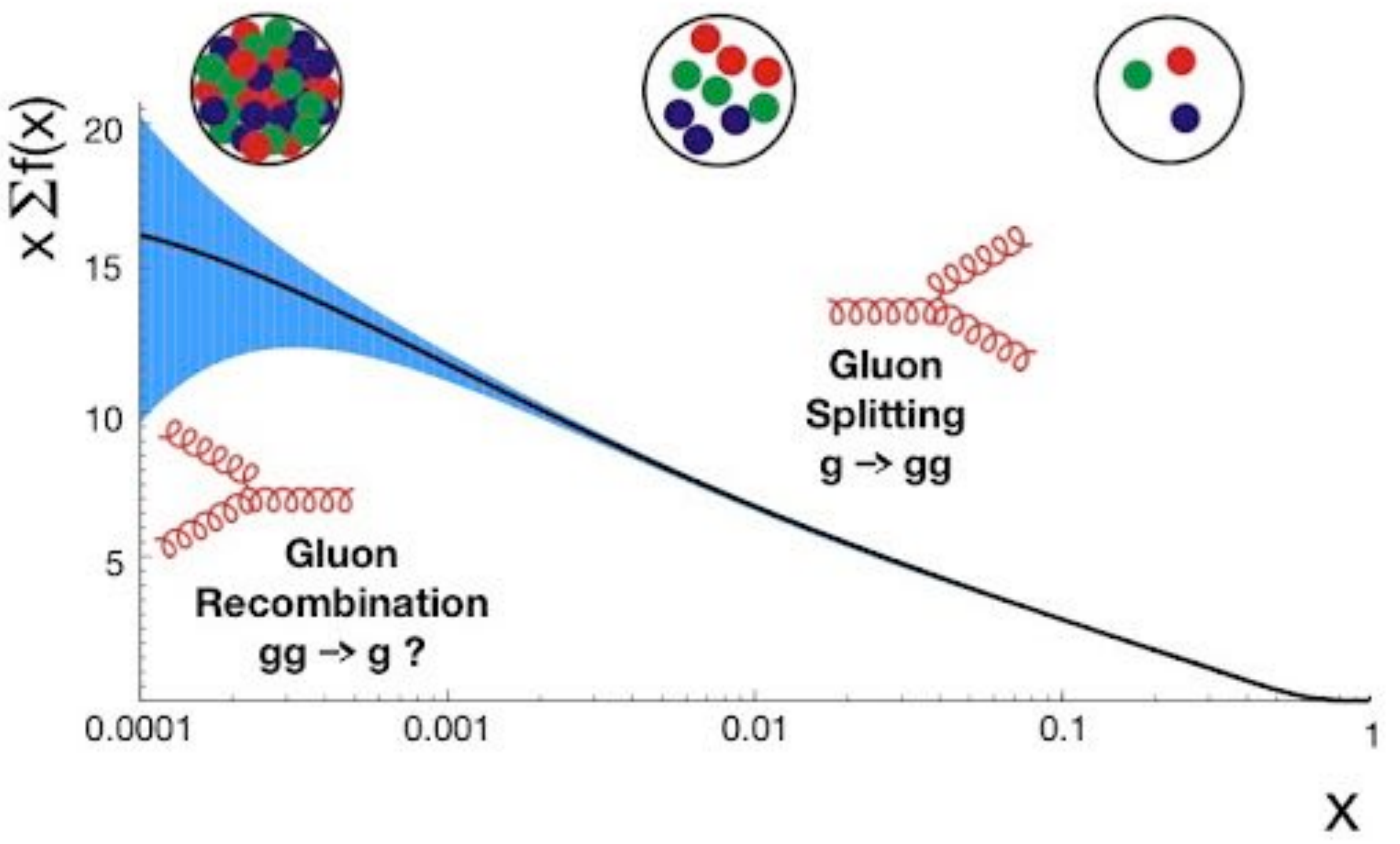

$$\sigma_{q\bar{q},N} \sim g^2(x)$$

Sensitive to small x gluons!

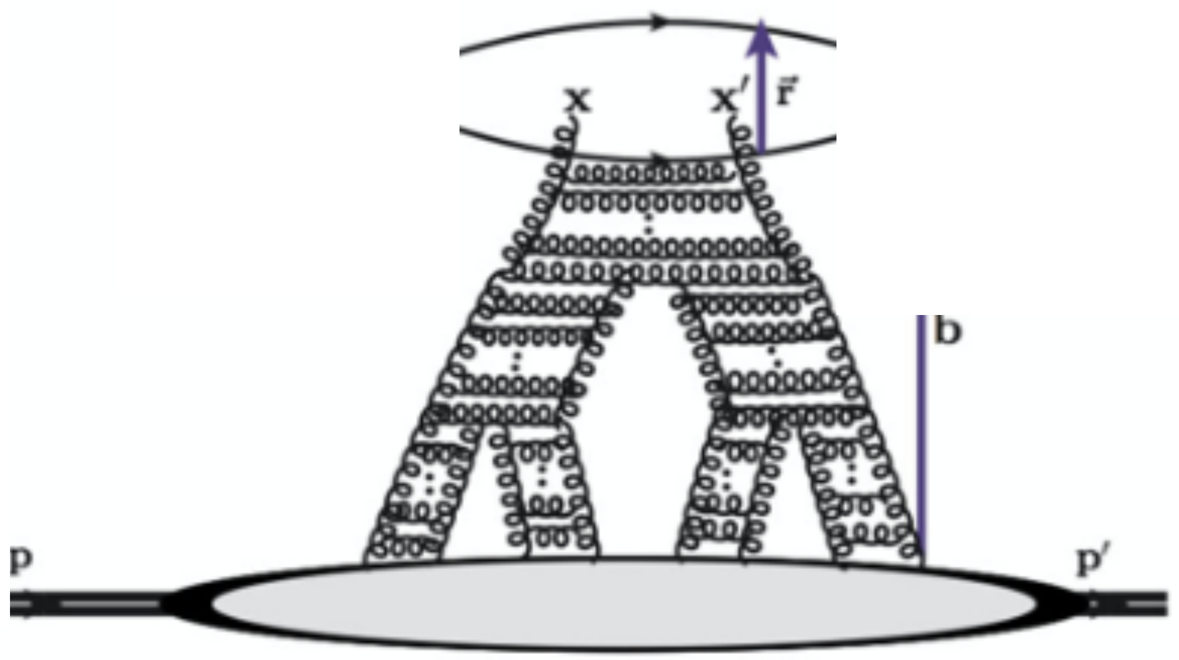

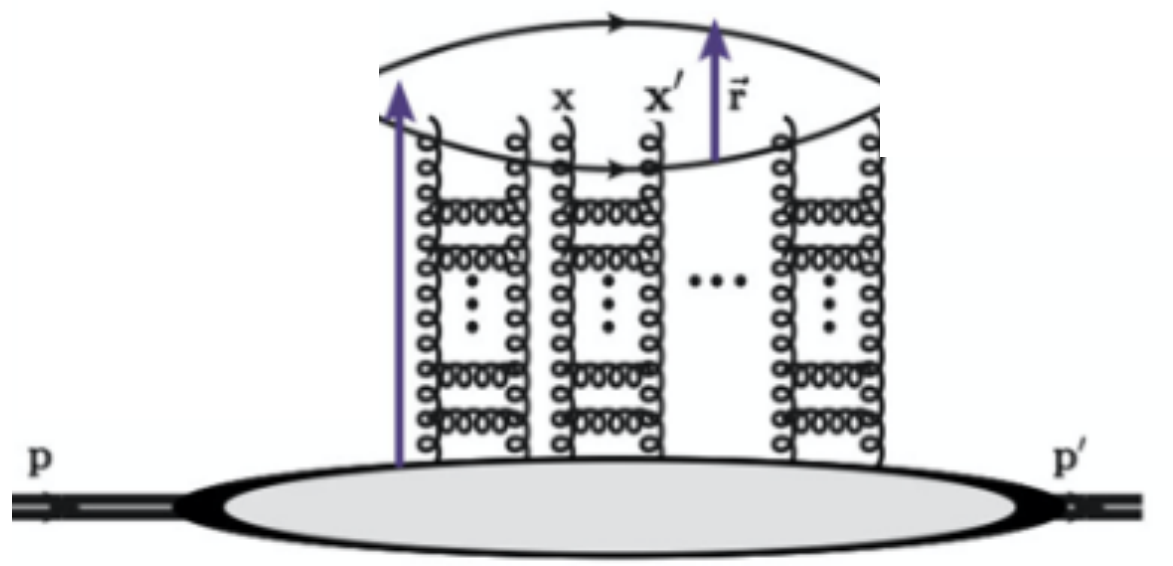

Nonperturbative, contains the gluon saturation information.

- Traditionally, model parameters are introduced in every element and then fitted to data (around 300 data points).

- To extract the gluon saturation information (encoded in $\sigma_{q\bar{q},N}$) from experiment data, it is helpful to determine the $q\bar{q}$-LFWFs of vector meson and photon as accurate as possible.

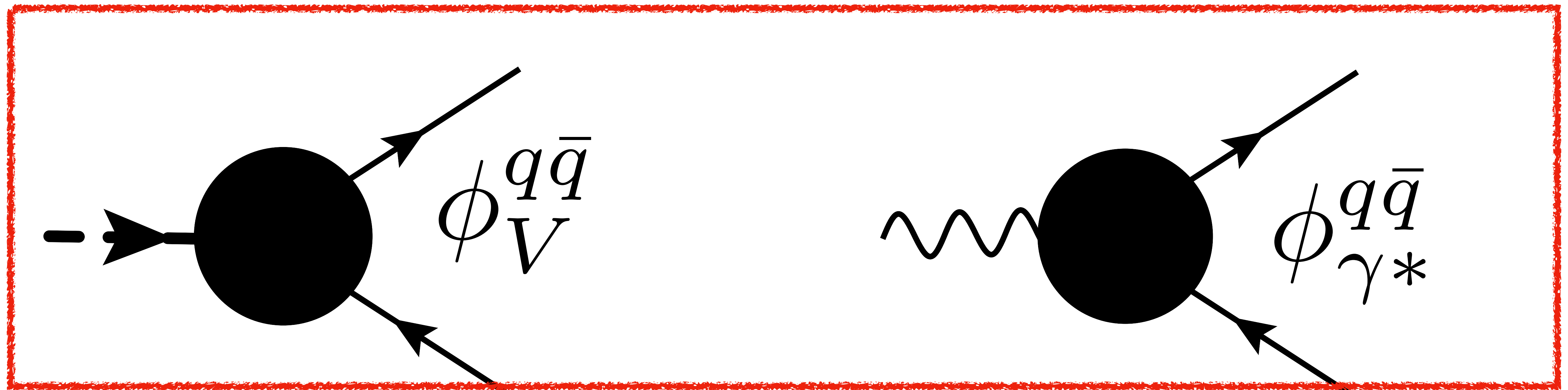

Light Front space-time

Instant Form & Front Form

$$x^0 \to x^+ = \frac{x^0 + x^3}{\sqrt{2}}, \qquad x^3 \to x^- = \frac{x^0 - x^3}{\sqrt{2}}$$

P. A. M. Dirac, Forms of relativistic dynamics, Rev. Mod. Phys. 21, 392 (1949)

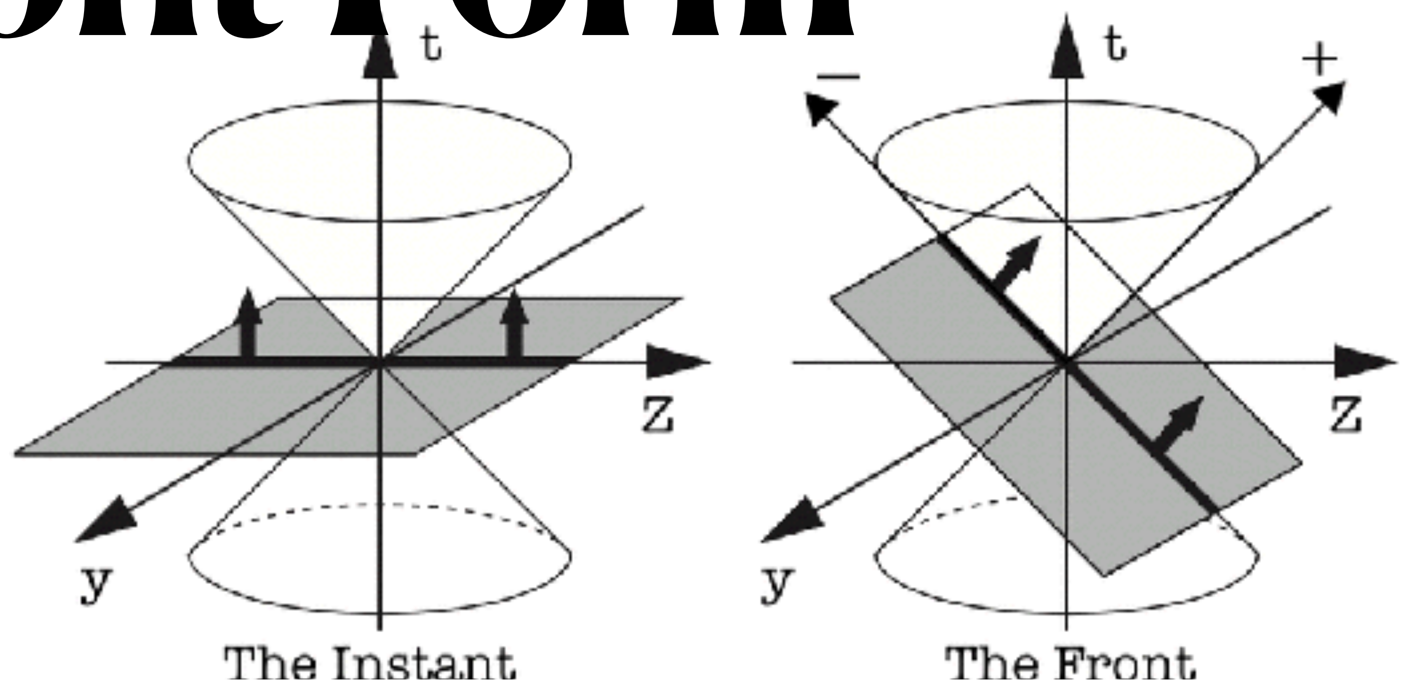

Dynamics at Infinite Momentum*

Steven Weinberg

Department of Physics, University of California, Berkeley, California†

(Received 6 June 1966)

- It is space-time re-parameterization.
- It is NOT reference frame.
- Yet front form is closely related to the infinite momentum frame.

PHYSICAL REVIEW VOLUME 180, NUMBER 5 25 APRIL 1969

Feynman Rules and Quantum Electrodynamics at Infinite Momentum

Shau-Jin Chang* and Shang-Keng Ma†

We have studied the Feynman rules in terms of the new variables $s = p^0 - p^3$, $\eta = p^0 + p^3$, and $\mathbf{q} = (p^1, p^2)$ in the ϕ^3 model and in quantum electrodynamics. The connection between the new variables and the dynamics at infinite momentum is established. In the ϕ^3 model, one easily deduces Weinberg's rules at infinite mo-

From BSA to LFWFs $\langle b^+_{\lambda,f} d^+_{\lambda',g} | \rho, J/\psi, \gamma \rangle$

"...'t Hooft did not use the light–cone formalism and which nowadays might be called standard. Instead, he started from covariant equations... The light–cone Schrodinger equation was then obtained by projecting the Bethe–Salpeter equation onto hyper-surfaces of equal light–cone time." (T. Heinzl arXiv:hep-th/0008096)

$$\int \frac{dk^-}{2\pi} \Psi_{BS}(k;p) = \frac{u^{(1)}(x_1, k_\perp)}{\sqrt{x_1}} \frac{u^{(2)}(x_2, -k_\perp)}{\sqrt{x_2}} \psi(x_1, k_\perp)$$

(G. Lepage and S. Brodsky, PRD 1980)

$$\psi(x, \mathbf{p}; s_1, s_2) = \frac{1}{2P^+} \int \frac{dp^-}{2\pi} \, \bar{u}(xP^+, \mathbf{p}; s_1)\gamma^+ \Phi(p) \gamma^+ v((1-x)P^+, -\mathbf{p}; s_2) \, .$$

(H. Liu and D. Soper, PRD1993)

$$\langle 0|\bar{d}_+(0)\gamma^+\gamma_5 u_+(\xi^-, \xi_\perp)|\pi^+(P)\rangle = i\sqrt{6}P^+\psi_0(\xi^-, \xi_\perp),$$
$$\langle 0|\bar{d}_+(0)\sigma^{+i}\gamma_5 u_+(\xi^-, \xi_\perp)|\pi^+(P)\rangle = -i\sqrt{6}P^+\partial^i\psi_1(\xi^-, \xi_\perp).$$

(M. Burkardt, X. Ji, F. Yuan, PLB 2002)

$$\phi_i(x, \vec{k}_T) \sim \int dk^- dk^+ \delta(xP^+ - k^+) \mathrm{Tr}[\Gamma_i \chi(k, P)]$$

(C.S., Ya-ping Xie, M Li, Xurong Chen, Hongshi Zong, PRD(L) 2021)

The Projection Formula

Covariant Bethe-Salpeter wave function

$$\underbrace{\phi_i(x,\vec{k}_T)}_{\text{LFWF}} \sim \int \underbrace{dk^-}_{\text{Setting light front time } \xi^+=0} \underbrace{dk^+\delta(xP^+ - k^+)}_{\text{set } k^+ = xP^+} \mathrm{Tr}[\underbrace{\Gamma_i}_{\text{spin configurations}} \chi(k,P)]$$

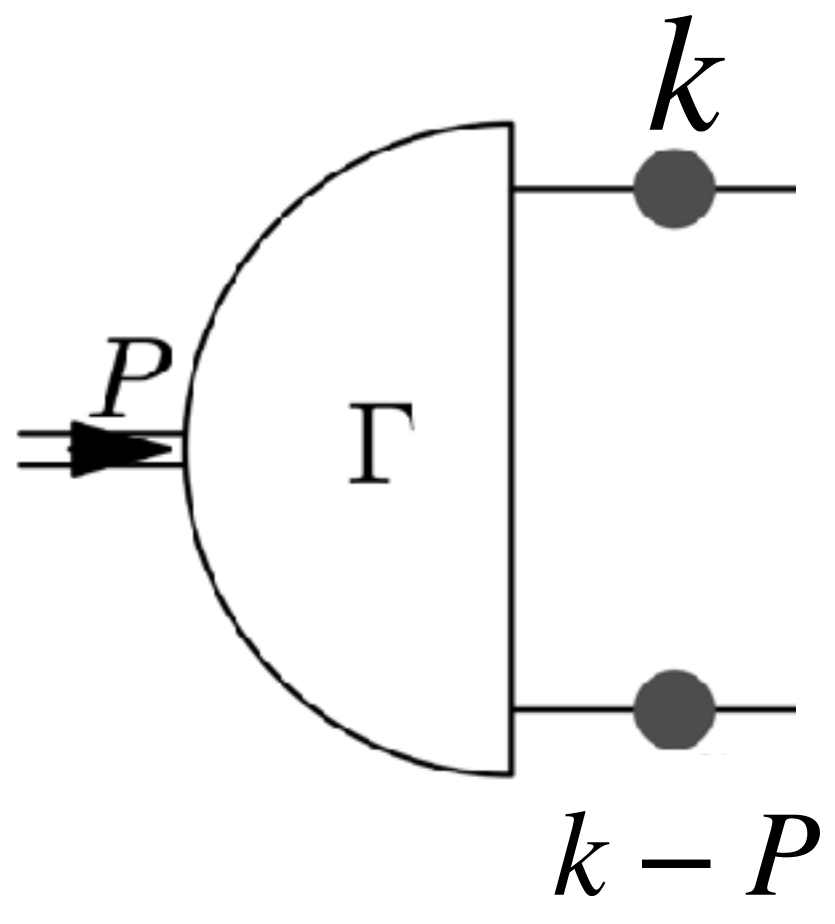

spin configurations

LFWF

set $k^+ = xP^+$

Setting light front time $\xi^+ = 0$

Bethe-Salpeter equations for vector meson and photon

Vector Meson BSE:

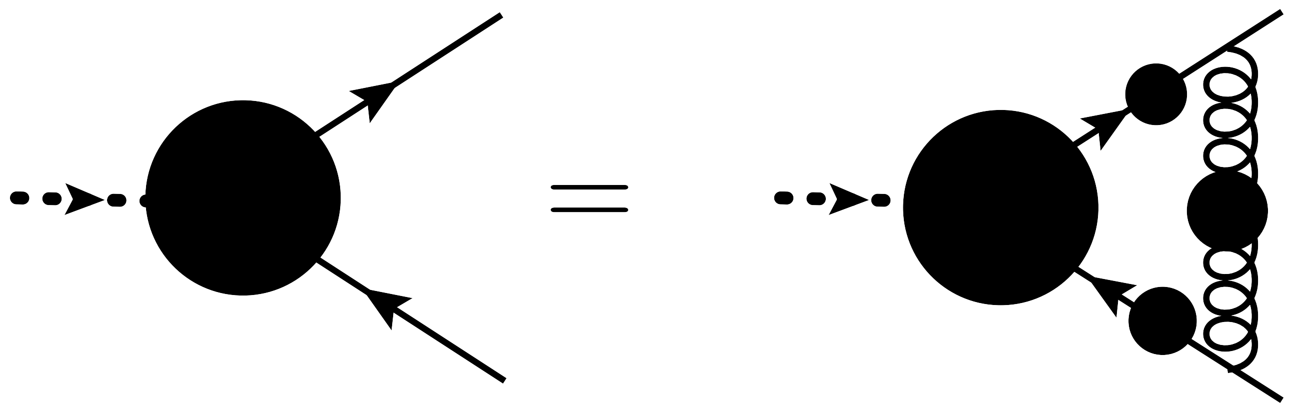

Photon BSE:

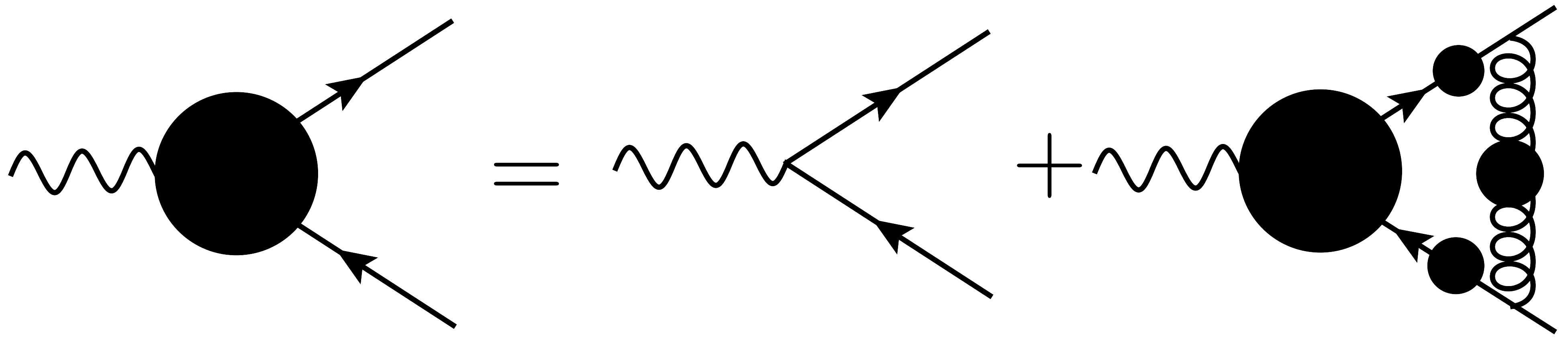

Align with quark's DSE:

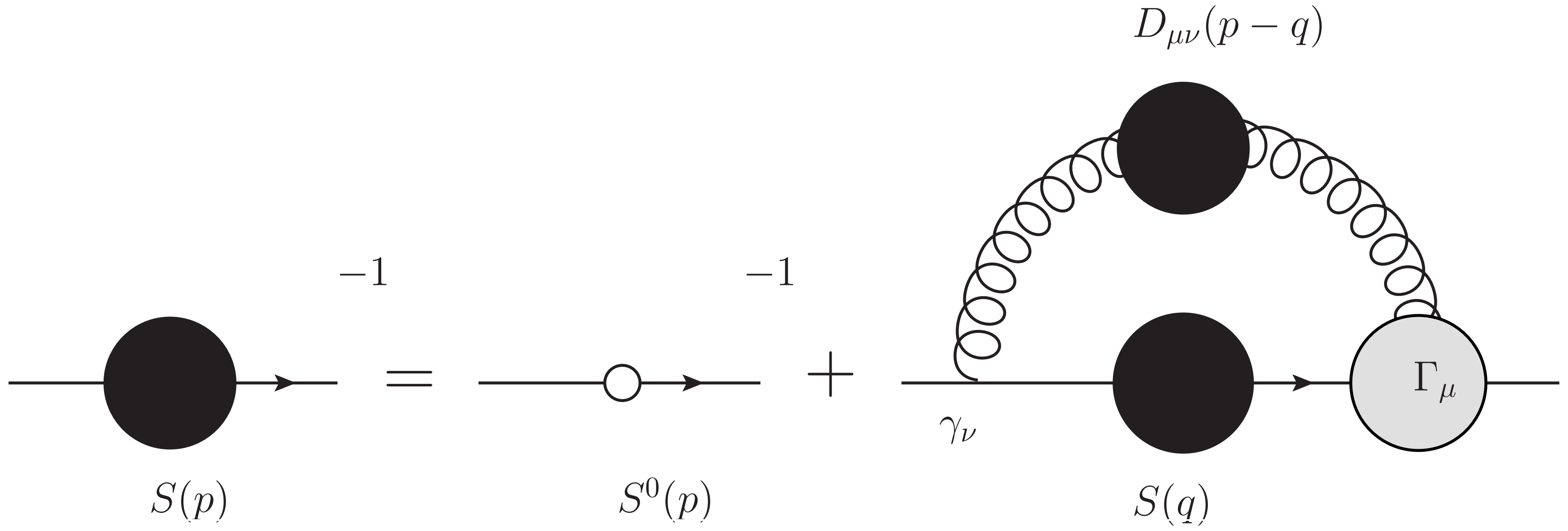

- Rainbow-Ladder & Maris-Tandy model (2 parameters)
- Preserve chiral symmetry.
- Fruitful predictions on ground states spectrum, form factors and parton distributions.

General Analysis for 1^- Meson

BS WFs

$$\chi_\mu^M(k,P) = \sum_{i=1}^8 T_\mu^i(k,P)\boxed{F^i(k^2, k\cdot P, P^2)}$$

$$A_1 = k_\mu - \frac{P_\mu P\cdot k}{P^2},\; A_2 = \gamma_\mu - \frac{P_\mu \not{P}}{P^2},$$
$$B_1 = I_4,\; B_2 = \not{P},\; B_3 = \not{k},\; B_4 = [\not{k}, \not{P}],$$

$$T_\mu^1 = iA_1.B_1, \qquad T_\mu^2 = A_1.B_2(k\cdot P),$$
$$T_\mu^3 = A_1.B_3, \qquad T_\mu^4 = -iA_1.B_4,$$
$$T_\mu^5 = A_2.B_1, \qquad T_\mu^6 = -iA_2.B_2,$$
$$T_\mu^7 = -i[A_2, B_3](k\cdot P),\; T_\mu^8 = \{A_2, B_4\}\,.$$

8 Lorentz scalar functions

LF-LFWFs

$$|M\rangle^\Lambda = \sum_{\lambda,\lambda'}\int \frac{d^2\boldsymbol{k}_T}{(2\pi)^3}\frac{dx}{2\sqrt{x\bar{x}}}\frac{\delta_{ij}}{\sqrt{3}}$$
$$\Phi^\Lambda_{\lambda,\lambda'}(x,\boldsymbol{k}_T)\, b^\dagger_{f,\lambda,i}(x,\boldsymbol{k}_T)\, d^\dagger_{f,\lambda',j}(\bar{x},\bar{\boldsymbol{k}}_T)|0\rangle.$$

$$\Phi^0_{\pm,\mp} = \boxed{\psi^0_{(1)}}, \qquad \Phi^0_{\pm,\pm} = \pm k_T^{(\mp)}\boxed{\psi^0_{(2)}};$$
$$\Phi^{\pm1}_{\pm,\pm} = \boxed{\psi^1_{(1)}}, \qquad \Phi^{\pm1}_{\pm,\mp} = \pm k_T^{(\pm)}\boxed{\psi^1_{(2)}};$$
$$\Phi^{\pm1}_{\mp,\pm} = \pm k_T^{(\pm)}\boxed{\psi^1_{(3)}},\; \Phi^{\pm1}_{\mp,\mp} = (k_T^{(\pm)})^2\boxed{\psi^1_{(4)}}$$

(X. Ji, J.-P. Ma, F. Yuan, EPJC2004)

6 independent scalar functions,
reduce to 5 for G-parity eigenstate

Vector meson LF-LFWFs

$$\Lambda = \lambda + \lambda' + L_z$$

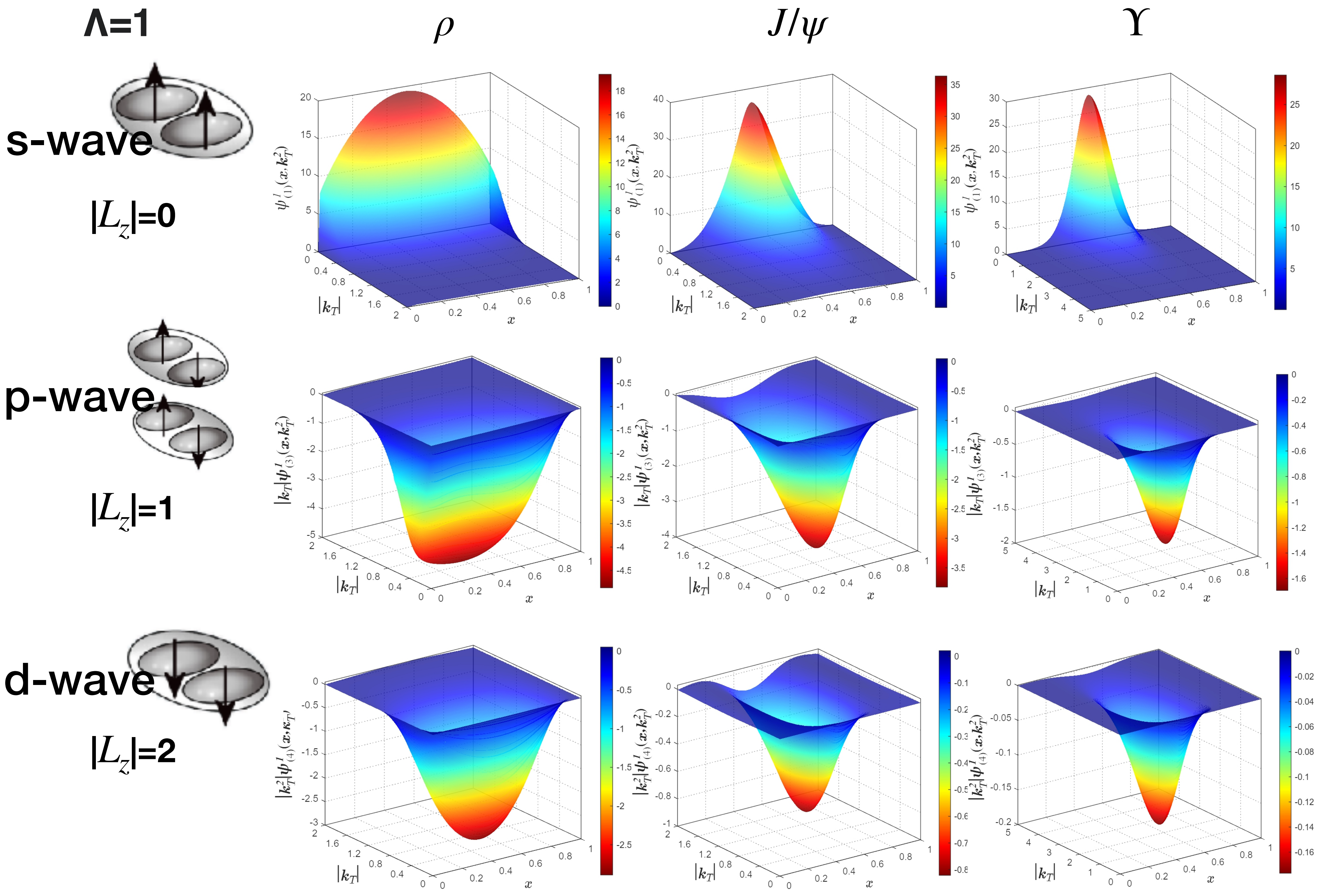

(CS, Jicheng Li, et al, PRD2022)

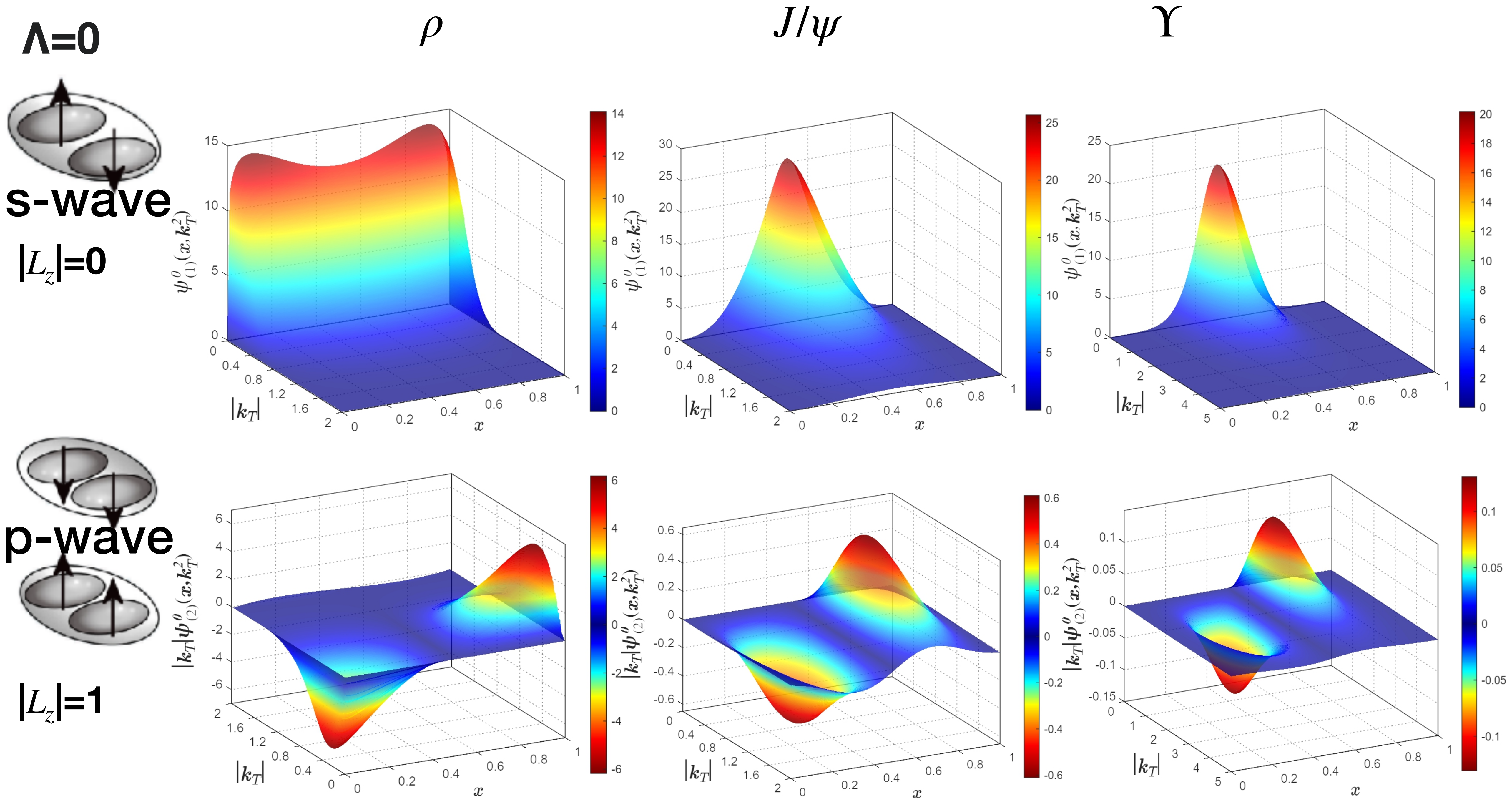

- All nonvanishing

Leading Fock-state VS Higher Fock-state

$$|M\rangle = \phi_2 | q\bar{q}\rangle + \phi_3 | q\bar{q}g\rangle + \phi_4 | q\bar{q}q\bar{q}\rangle + \ldots$$

HF=Higher Fock states

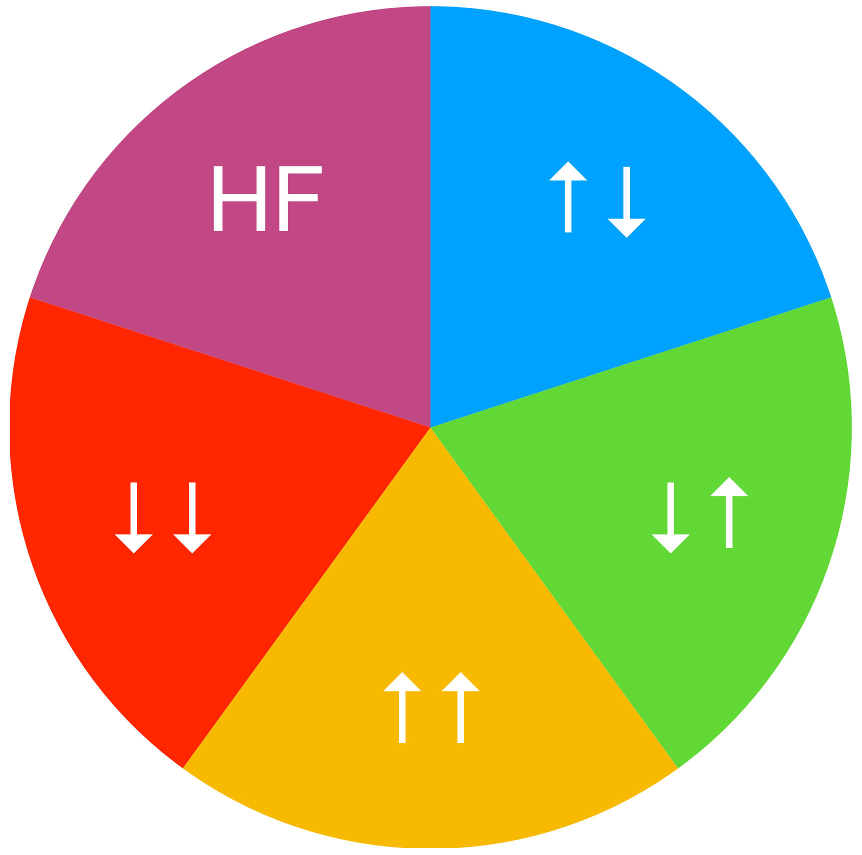

BSWF Norm

$$G_4(p,q;P) = \Sigma_i \frac{\chi_i(p,P_i)\bar{\chi}_i(q,-P_i)}{P^2 - P_i^2} + R(p,q;P)$$

$$\langle M | M\rangle = 1$$

LFWF Norm

$$\sum_{n,\lambda_i} \int \overline{\prod_i} dx_i \frac{d^2 k_{\perp i}}{16\pi^3} |\psi_{n/\pi}(x_i, \mathbf{k}_{\perp i}, \lambda_i)|^2 = 1\,.$$

- But we only calculated $q\bar{q}$ component.

$\rho^{\Lambda=0}$

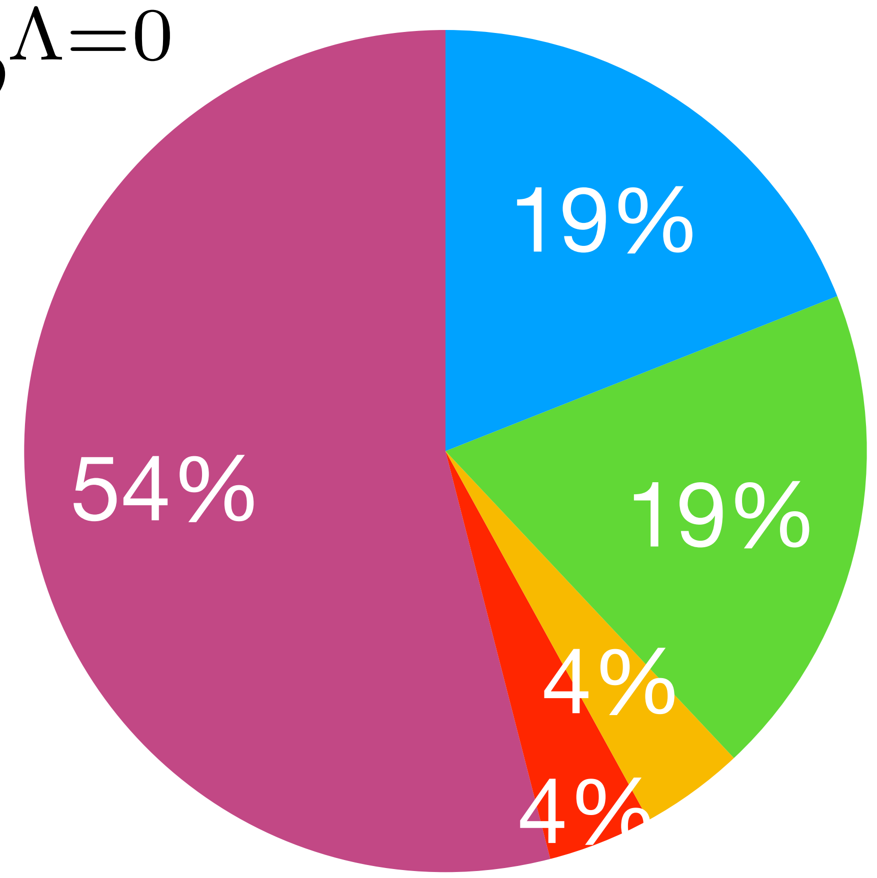

$\rho^{\Lambda=1}$

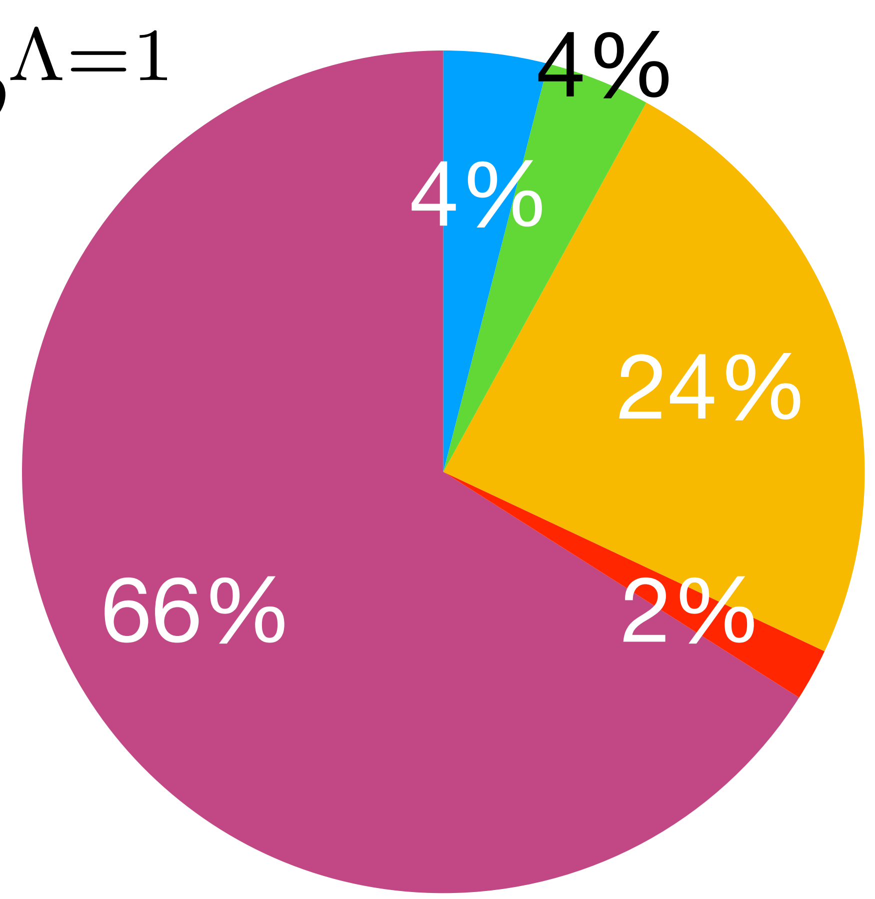

$J/\psi^{\Lambda=0}$

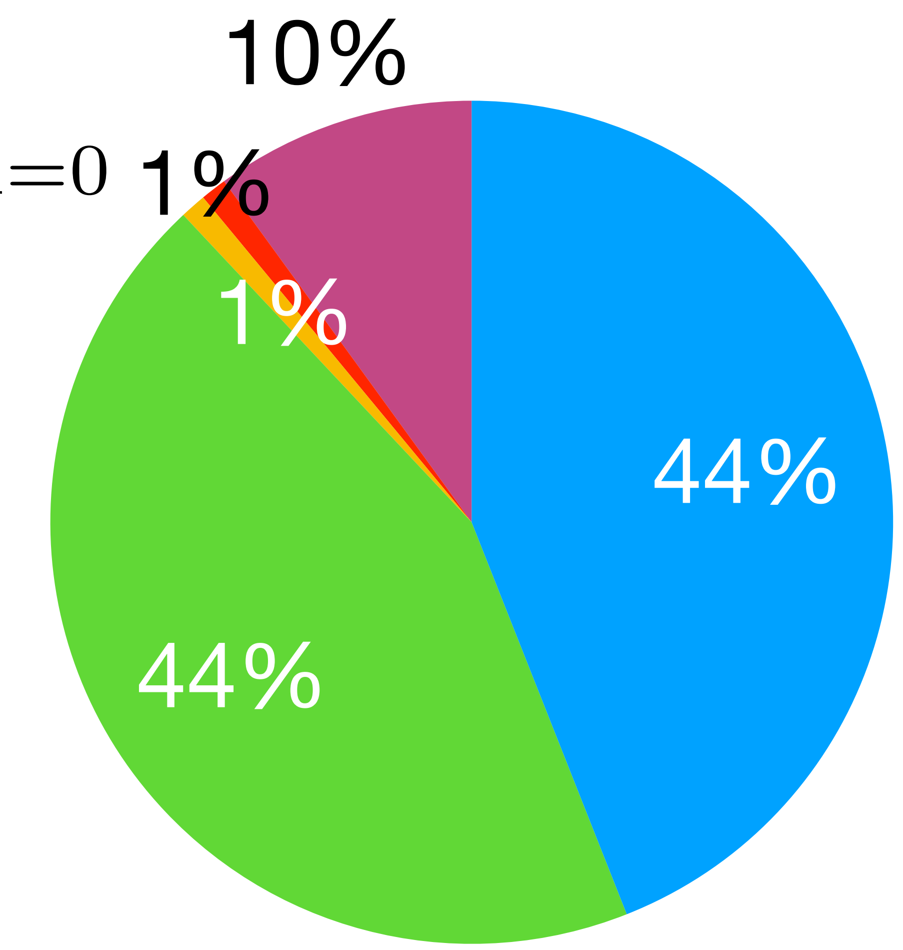

$J/\psi^{\Lambda=1}$

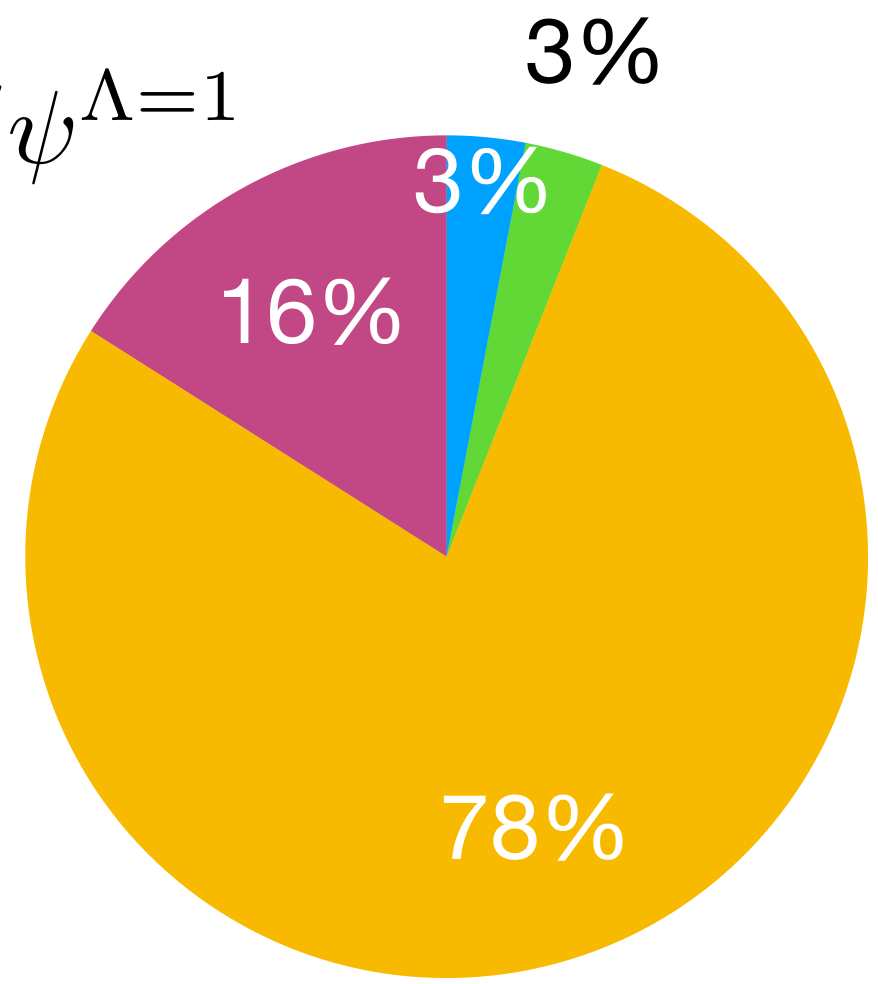

- There are significant higher Fock states contribution in ρ, and reduces in heavier J/ψ.

Diffractive Vector meson Production

$$\sigma \sim \phi_{\gamma^*}^{q\bar{q}} \otimes \sigma_{q\bar{q},N} \otimes \phi_V^{q\bar{q}}$$

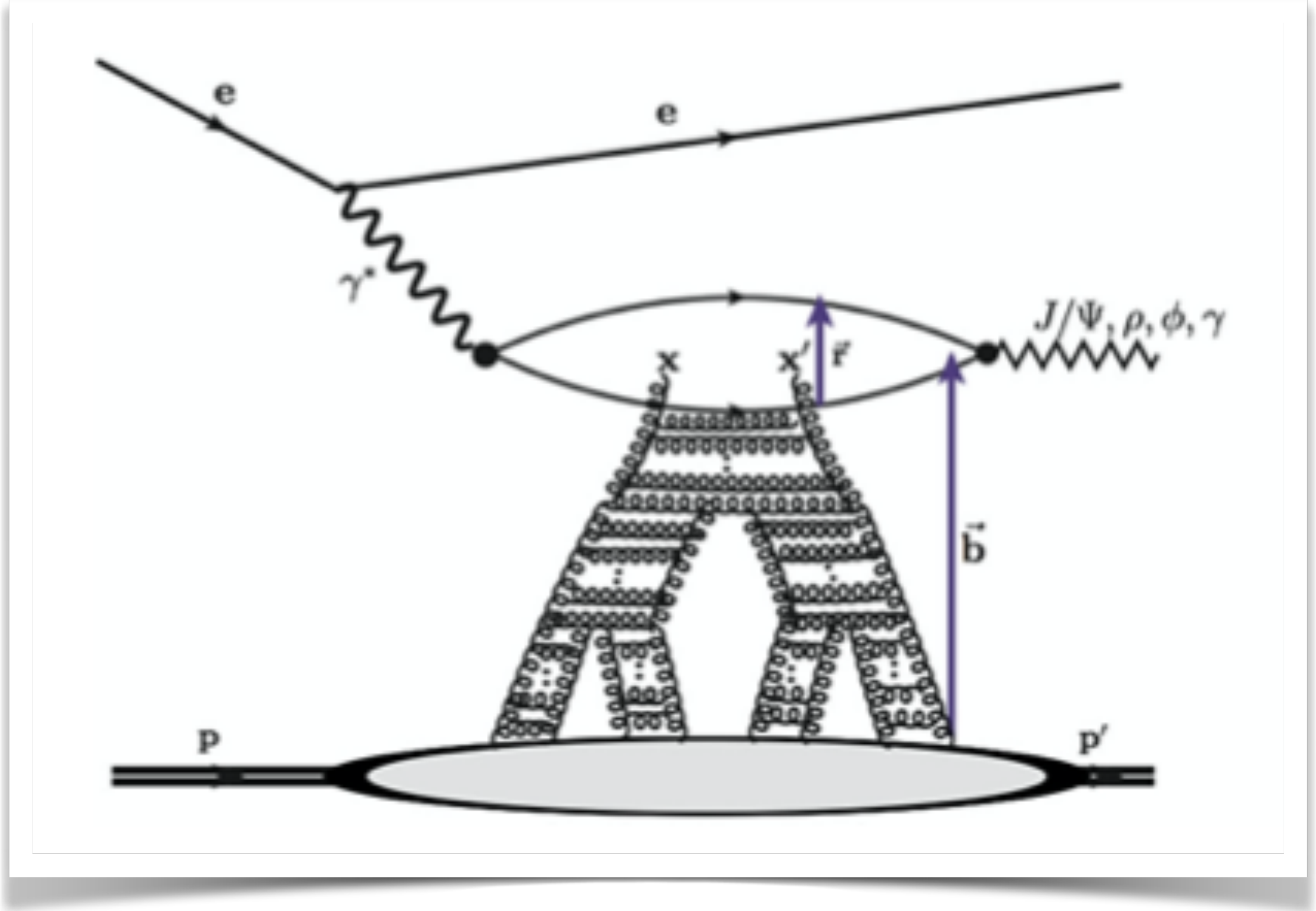

$\phi_{\gamma *}^{q\bar{q}}$ LO QED Light-cone perturbation/$m_f = 140$MeV

$\sigma_{q\bar{q},N}$ bCGC model

$$\sigma_{q\bar{q}}^{\mathrm{CGC}}(x,r) = \sigma_0 \times \begin{cases} \mathcal{N}_0 \left(\frac{rQ_s}{2}\right)^{2(\gamma_s + (1/\kappa\lambda Y)\ln(2/rQ_s))} & : rQ_s \le 2 \\ 1 - \mathrm{e}^{-A\ln^2(BrQ_s)} & : rQ_s > 2 \end{cases},$$

BFKL

Balitsky-Kovchegov

$\phi_V^{q\bar{q}}$ BSEs-LFWFs Our prediction

Result

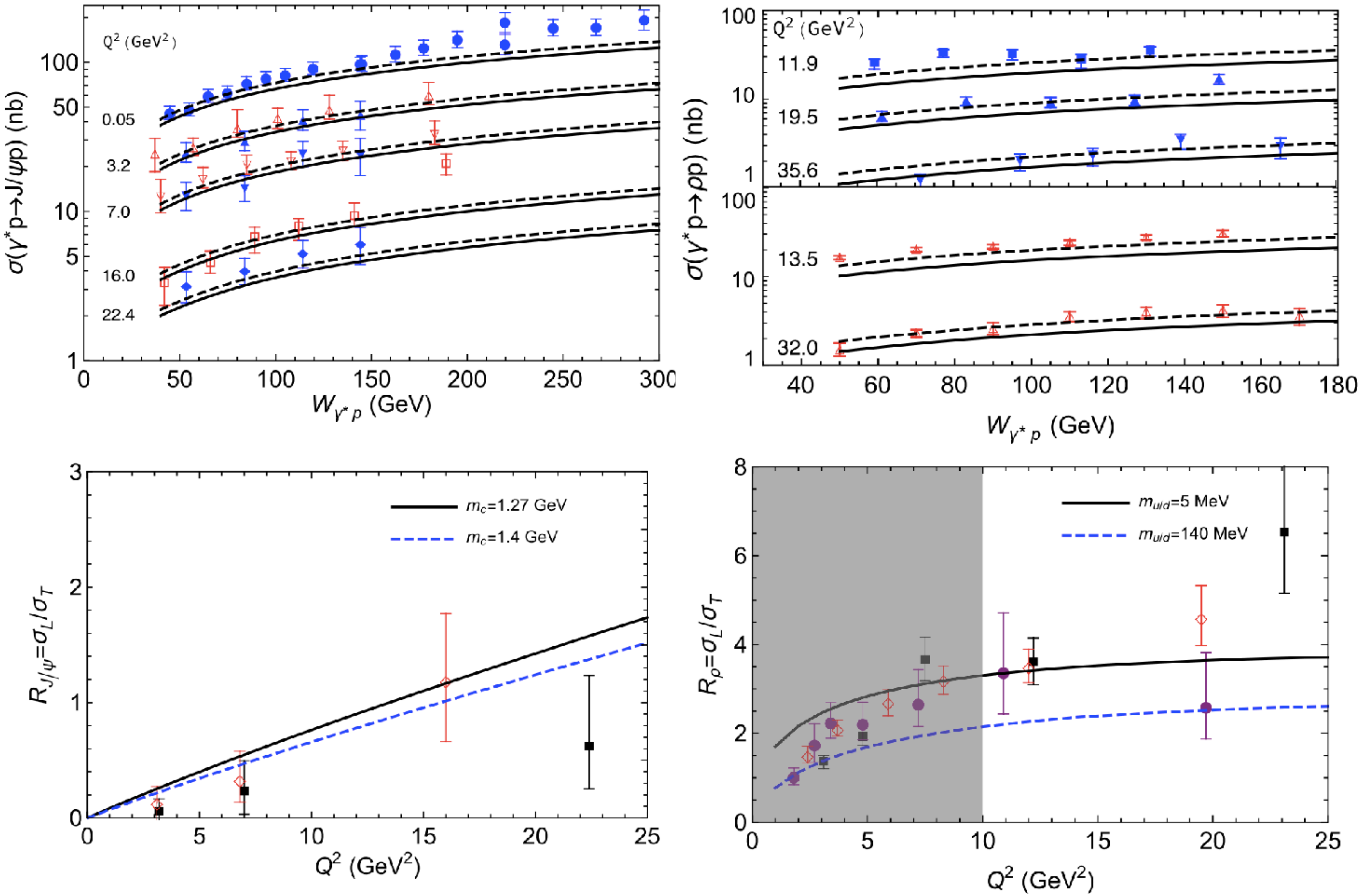

- In agreement with HERA data.
- Our LFWFs are very different from models employed by color dipole model studies before!

(C.S., Ya-Ping Xie, Ming Li, Xurong Chen and Hong-Shi Zong, PRD(L)2021)

Photon Bethe-Salpeter wave function

$$\sigma \sim |\phi_{\gamma^*}^{q\bar{q}}|^2 \otimes \sigma_{q\bar{q},N}$$

$$\sigma \sim \phi_{\gamma^*}^{q\bar{q}} \otimes \sigma_{q\bar{q},N} \otimes \phi_V^{q\bar{q}}$$

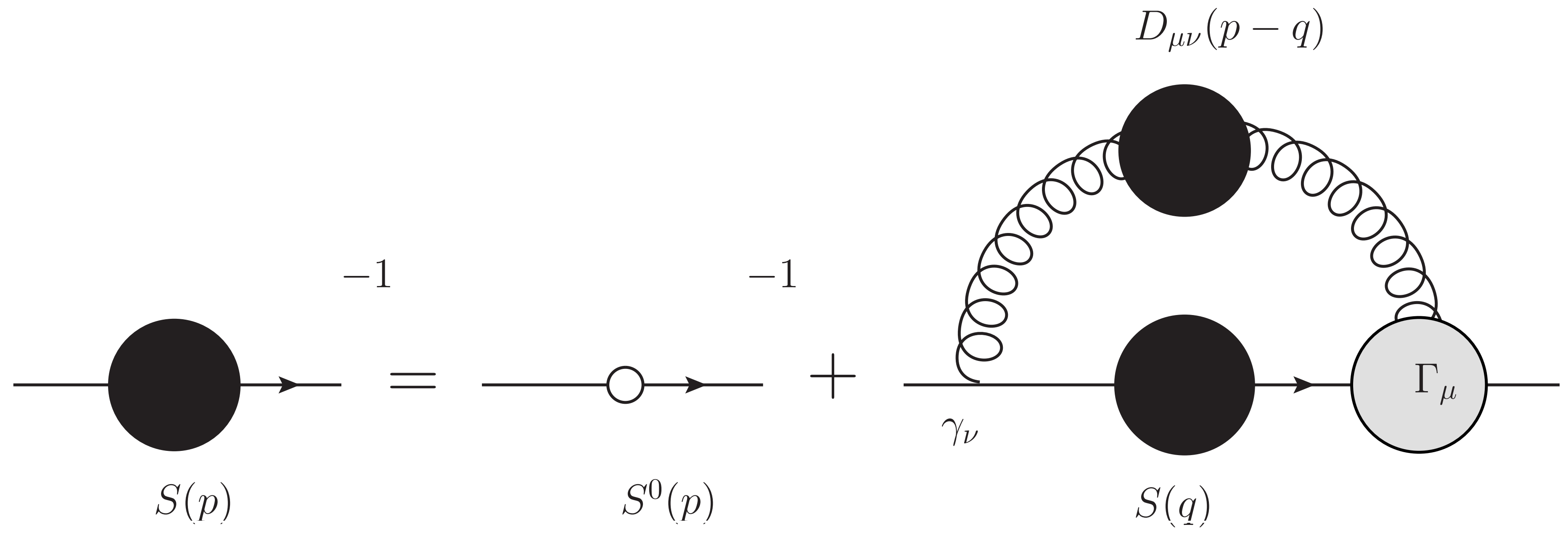

$$S_f^{-1}(k) = i\gamma \cdot k + m_f + \frac{4}{3}\frac{4\pi\alpha_{\mathrm{IR}}}{m_G^2}\int \frac{d^4q}{(2\pi)^4}\gamma_\mu S_f(q)\gamma_\mu,$$

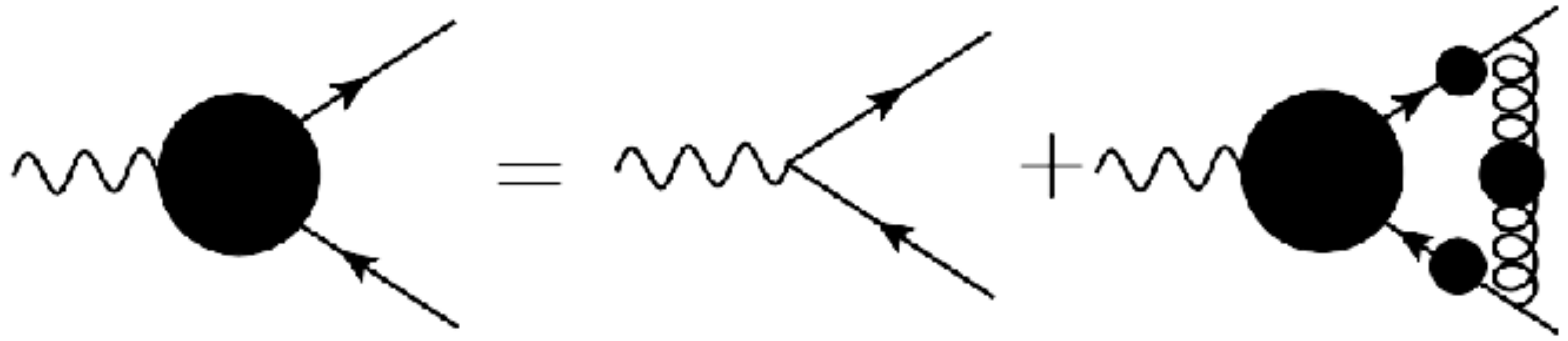

$$\Gamma_\mu^{\gamma^*,(f)}(k;Q) = \gamma_\mu - \frac{4}{3}\frac{4\pi\alpha_{\mathrm{IR}}}{m_G^2}\int \frac{d^4q}{(2\pi)^4} \times \gamma_\alpha S_f(q)\Gamma_\mu^{\gamma^*,(f)}(q;Q)S_f(q-Q)\gamma_\alpha,$$

Contact interaction Model: $g^2 D_{\mu\nu}(k-q) = \delta_{\mu\nu}\frac{4\pi\alpha_{\mathrm{IR}}}{m_G^2}$

$$S_f(p)^{-1} = i\gamma \cdot p + M_f, \qquad \Gamma_\mu^{\gamma^*,(f)}(Q) = \gamma_\mu^T P_T^{(f)}(Q^2) + \gamma_\mu^L P_L^{(f)}(Q^2)$$

Photon LFWF

$$\Phi^{\Lambda,(f)}_{\lambda,\lambda'}(x,\boldsymbol{k}_T) = -\frac{1}{2\sqrt{3}}\int\frac{dk^-dk^+}{2\pi}\delta(xQ^+ - k^+)\mathrm{Tr}\left\{\Gamma_{\lambda,\lambda'} \quad S_f(k)[e_f e\Gamma^{\gamma^*,(f)}(k;Q)\cdot\epsilon_\Lambda(Q)]S_f(k-Q)\right\}$$

$$\langle x\rangle^m \equiv \int_0^1 dx x^m \underline{\Phi^0_{+,-}(x,\boldsymbol{k}_T)}$$

$$= -\frac{e_f e P_T(Q^2)}{2\sqrt{3}}\int\frac{d^2\boldsymbol{k}_\parallel}{2\pi}\left(\frac{k^+}{Q^+}\right)^m\frac{1}{|Q^+|}\mathrm{Tr}\left[(I+\gamma^5)\gamma^+ S(k)[\Gamma^{\gamma^*}(k;Q)\cdot\epsilon_0(Q)]S(k-Q)\right]$$

$$= -\frac{e_f e P_T(Q^2)}{2\sqrt{3}|Q\cdot n|}\int\frac{d^2\boldsymbol{k}_\parallel}{2\pi}\left(\frac{k_\parallel\cdot n}{Q\cdot n}\right)^m\frac{\mathrm{Tr}[\not{n}(-i\not{k}+M)\epsilon_0(-i\not{k}+i\not{Q}+M)]}{(k^2+M^2)(k^2-2k\cdot Q+Q^2+M^2)}$$

$$= \frac{2\sqrt{N_c}e_f e P_T(Q^2)}{Q}\int_0^1 du' u'^m\int\frac{d^2\boldsymbol{k}_\parallel}{2\pi}\frac{k_\perp^2+M^2-u'(1-u')Q^2}{[k_\parallel^2+Q^2u'(1-u')+M^2+k_\perp^2]^2}$$

$$= \int_0^1 du' u'^m \underline{\frac{\sqrt{N_c}e_f e P_T(Q^2)}{Q}\left(1-\frac{2u'(1-u')Q^2}{Q^2u'(1-u')+M^2+k_\perp^2}\right)}.$$

Photon LFWF

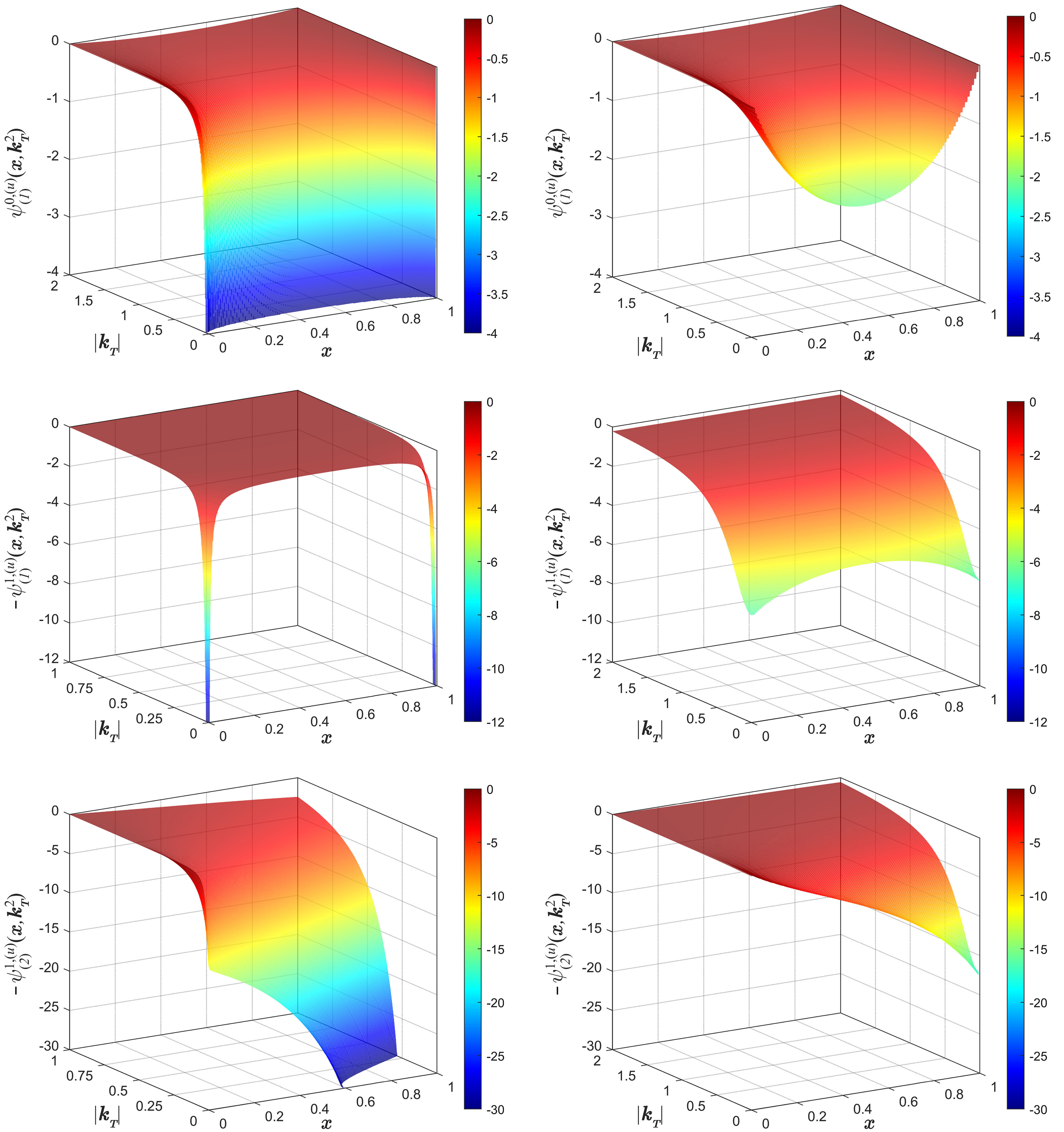

- $Q^2 \approx -(0.5\text{GeV})^2$
- Big difference between the perturbative (left) and nonperturbative (right) result.
- limited to low virtuality due to the simplified contact interaction model.
- high OAM LFWFs are missing due to contact interaction model.

Photon LFWF& small-x DIS

- DIS at small x

C. S., Z. Yang, Xurong Chen, C. Luo, Wenchang Xiang, PRD2024

$$\sigma \sim |\phi_{\gamma^*}^{q\bar{q}}|^2 \otimes \sigma_{q\bar{q},N}$$

- Introduce the nonperturbative photon LFWFs by interpolating between perturbative

$$|\Psi'^{(f)}_{T,L}(r,z;Q^2)|^2 = F_{\rm part}(Q^2)|\Psi^{(f),{\rm np}}_{T,L}(r,z;Q^2)|^2 + [1 - F_{\rm part}(Q^2)]|\Psi^{(f),{\rm p}}_{T,L}(r,z;Q^2)|^2$$

$$F_{\rm part}(Q^2) = \frac{Q_0^{2n}}{(Q^2+Q_0^2)^n}.$$

- fitting HERA data for x<0.01.

$$\sigma_r(x,y,Q^2) = F_2(x,Q^2) - \frac{y^2}{1+(1-y)^2}F_L(x,Q^2)$$

LFWFs [Eqs. (30-35,49)]	Q^2/GeV^2	γ_s	N_0	x_0	λ	Q_0^2	n	$\chi^2/\mathrm{d.o.f}$
Pert.	[0.85, 50]	0.6290	0.4199	2.395×10^{-4}	0.1962	-	-	265.8/223 = 1.192
Pert.	[0.25, 50]	0.3869	0.7556	7.047×10^{-7}	0.1052	-	-	678.4/282 = 2.406
Pert.+Nonpert.	[0.25, 50]	0.6177	0.4596	1.326×10^{-4}	0.1875	1.052	3.970	337.9/280 = 1.207

$\sigma_{q\bar{q},N}$ model parameter $F_{\rm part}$ model parameter

- Incorporating nonperturbative QCD into photon LFWFs significantly improve low Q^2 calculation.
- npQCD in photon LFWFs impacts $\sigma_{q\bar{q},N}$ determination, hence saturation information extraction.

Summary

- We generalize the light front projection method to the case of vector particle LFWFs, and used on modern DS-BSE solutions.
- The normalization examination indicates significant higher Fock-states lies in light meson.
- Determining the vector meson and photon LFWFs can help study the gluon saturation effect by constraining $\sigma_{q\bar{q},N}$

Outlook

- Refine photon LFWFs with realistic DS-BSEs to further constrain $\sigma_{q\bar{q},N}$.
- Radially excited mesons, strange quark, etc,...
- UPC, EIC, EicC, etc...

Thank you for listening!

Backup slides

- A covariant Feynman diagram contains many Fock states.
- "we study in light-front dynamics the contributions of dif- ferent Fock sectors (with increasing number of exchanged particles) to full normalization integral and electromagnetic form factor. "

ELSEVIER

Available online at www.sciencedirect.com
SCIENCE DIRECT

NUCLEAR PHYSICS B

Nuclear Physics B 696 [FS] (2004) 413–444

www.elsevier.com/locate/npe

Many-body Fock sectors in Wick–Cutkosky model

Dae Sung Hwang [a], V.A. Karmanov [b]